Optical and electro-optic anisotropy of epitaxial PZT thin films

Minmin Zhu, Zehui Du, Lin Jing, Alfred Iing Yoong Tok, and Edwin Hang Tong Teo

Citation: Applied Physics Letters **107**, 031907 (2015); doi: 10.1063/1.4927404
View online: http://dx.doi.org/10.1063/1.4927404
View Table of Contents: http://scitation.aip.org/content/aip/journal/apl/107/3?ver=pdfcov
Published by the AIP Publishing

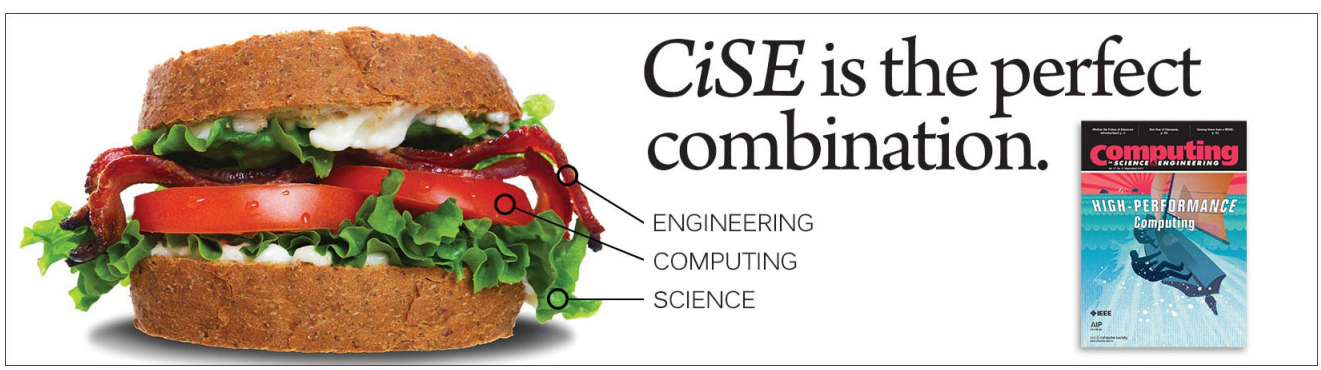

Optical and electro-optic anisotropy of epitaxial PZT thin films

Minmin Zhu,[1,2,3] Zehui Du,[4] Lin Jing,[5] Alfred Iing Yoong Tok,[5] and Edwin Hang Tong Teo[1,2,3,a)]
[1]School of Electrical and Electronic Engineering, Nanyang Technological University, 50 Nanyang Avenue, Singapore 639798
[2]CINTRA CNRS/NTU/THALES, UMI 3288 and Research Techno Plaza, 50 Nanyang Drive, Border X Block, Level 6, Singapore 637553
[3]Silicon Technologies, Centre of Excellence, 50 Nanyang Avenue, Singapore 639798
[4]Temasek Laboratories, Research Techno Plaza, 50 Nanyang Drive, Singapore 637553
[5]School of Materials Science and Engineering, Nanyang Technological University, 50 Nanyang Avenue, Singapore 639798

(Received 9 June 2015; accepted 10 July 2015; published online 22 July 2015)

Strong optical and electro-optic (EO) anisotropy has been investigated in ferroelectric $Pb(Zr_{0.48}Ti_{0.52})O_3$ thin films epitaxially grown on Nb-$SrTiO_3$ (001), (011), and (111) substrates using magnetron sputtering. The refractive index, electro-optic, and ferroelectric properties of the samples demonstrate the significant dependence on the growth orientation. The linear electro-optic coefficients of the (001), (011), and (111)-oriented PZT thin films were 270.8, 198.8, and 125.7 pm/V, respectively. Such remarkable anisotropic EO behaviors have been explained according to the structure correlation between the orientation dependent distribution, spontaneous polarization, epitaxial strain, and domain pattern. © *2015 AIP Publishing LLC*. [http://dx.doi.org/10.1063/1.4927404]

Transparent ferroelectric oxides with perovskite phase exhibit the best known combination of high transparency, large refractive index, and excellent electro-optic (EO) effects in wide wavelengths from the visible to the near-infrared (IR) range,[1–3] thus attracting much attention in the research and development of various novel optical devices such as optical modulator, beam deflector, and optical switches.[4–6] Recently, great efforts have been made to epitaxial growth of the corresponding single crystal so as to obtain large linear EO coefficients. Such single crystal structure can efficiently reduce the light scattering caused by surface roughness and grain boundaries which are usually presented in polycrystalline films. It is also well known that optical tensors of the ferroelectric thin films, such as refractive index (n) and EO coefficient, are generally anisotropic because the spontaneous polarization has been switched due to the lattice distortion. Thus, fully understanding the optical and electro-optic anisotropy of such single crystal is not only of scientific interest but also of industrial importance.

$Pb(Zr_{1-x}Ti_x)O_3$ (PZT) thin film with a composition at morphotropic phase boundary (MPB, $x = 0.52$) has been found to have remarkable spontaneous polarization ($82\,\mu C/cm^2$),[7] high Curie temperature (450 °C),[8] and huge piezoelectric coefficient d_{33} (311 pC/N),[9] which make it a superior ferroelectric materials for multifunctional optoelectronic applications. Currently, there have been some efforts to study EO behaviors of single crystal PZT films on various substrates. Kurihara *et al.* found one small EO coefficient of ~76 pm/V in PZT films (100) epitaxially grown on Si wafer.[10] Kang *et al.* also reported one larger EO coefficient of ~134.6 pm/V in epitaxial-grown PZT thin film on Nb-$SrTiO_3$ (Nb-STO) (001) substrate.[11] Using $(Pb_{0.86}La_{0.14})TiO_3$ as the seeding layer, our previous study demonstrates the largest EO coefficient of PZT thin film as high as ~219 pm/V.[12] Although there are a few of EO anisotropy behaviors reported in some ferroelectric oxides, such as $(Ba_{0.7}Sr_{0.3})TiO_3$ and $Pb(Mg_{2/3}Nb_{1/3})O_3$-$PbTiO_3$,[13,14] information pertaining to optical and EO anisotropy of PZT thin films is still limited. Shinozaki *et al.* observed the difference on EO behavior of (101)- and (100)-oriented epitaxial PZT films on Si substrate, but the EO coefficient is very small and only around 60 pm/V.[15] More importantly, to date, no a systematic study on refractive index and electro-optic anisotropy of single crystal PZT films has been performed yet. In this letter, we investigated the optical, electro-optic, and ferroelectric properties of epitaxial single crystal PZT thin films according to their crystalline orientation. The underlying mechanism for optical and electro-optic anisotropy has also been discussed.

Polycrystalline $Pb(Zr_{0.48}Ti_{0.52})O_3$ ceramic disk plus 10% excess lead was selected for sputtering target due to easy lead evaporation. Orientation engineered PZT thin films with crystal orientations of (001), (011), and (111) have been epitaxially grown on highly transparent two-side polished single crystal Nb-$SrTiO_3$ (001), (011), and (111) substrates. The detailed deposition conditions in this work have been reported in our previous work.[12] The samples were post-annealed by rapid thermal processing (RTP) under oxygen atmosphere at 650 °C for 5 min to obtain high crystallinity. X-ray diffraction (XRD) and Atomic force microscopy (AFM) were performed to investigate the crystallinity and morphology of the as-grown PZT thin films. The optical properties of these samples were studied by spectroscopic ellipsometry VB-250 at wavelengths between 450 and 900 nm with 3 nm intervals. A modified ellipsometric measure setup using a 632.8 nm He–Ne laser was built to study the anisotropic EO behaviors of epitaxial PZT thin films. The polarization-electric field hysteresis loops were measured using a four probe workstation.

a)Author to whom correspondence should be addressed. Electronic mail: htteo@ntu.edu.sg

Nb-STO has been selected as a substrate material not only for one small lattice mismatch (3.4%)[16] but also for its excellent conductivity which makes it possible to be used as bottom electrodes in the ferroelectric and electro-optic measurements. Figs. 1(a)–1(c) show the typical XRD profiles of the PZT thin films grown on Nb-$SrTiO_3$ substrates with narrow diffraction peaks. It confirms that the PZT films epitaxially grown in (001), (011), and (111) Nb-STO substrates have been obtained. The films are with pure perovskite phase, and no secondary orientation or impurity phase has been detected from the $\theta/2\theta$ scanning. Meanwhile, X-ray rocking curve analysis (not shown) of the full width at half maximum (FWHM) has also been performed on these PZT thin films with remarkable growth orientation. The FWHM of these samples is 0.2°, 0.31°, and 0.37°, respectively. Such narrowness of the three peaks represents the films' high single crystalline quality from epitaxial growth. The in-plane texturing of the PZT thin films with respect to the major axes of the Nb-STO substrates was also confirmed by the XRD Phi-circle scan, as shown in Figs. 1(d)–1(f). The peaks from PZT films coincide in position well with those from Nb-STO substrates, which suggests a nonlattice-rotated epitaxial growth of all the as-grown PZT thin films.[14] Such epitaxial growth is desirable for optical applications since it can effectively reduce light scattering caused by grain boundary and surface roughness in thin films.

The surface roughness of PZT films has been measured by AFM, as shown in Fig. 2(a). The surface roughness is about 3.8 nm and no pores between irregular-shaped grains are observed, indicating that the films are very smooth and homogeneous. This can also help to minimize the light loss due to surface scattering. Fig. 2(b) shows the calculated refractive indices of the three epitaxial (001), (011), and (111)-oriented PZT films measured by spectroscopic ellipsometry over a wavelength range of 450–900 nm. The measure ellipsometric parameters Ψ and Δ in (001)-, (011)-, and (111)-oriented PZT films are shown in the inset of Fig. 2(b). It is noted that the number of oscillations depends on the thickness of the thin films. The refractive indices of the PZT films are extracted using Cauchy dispersion model given by

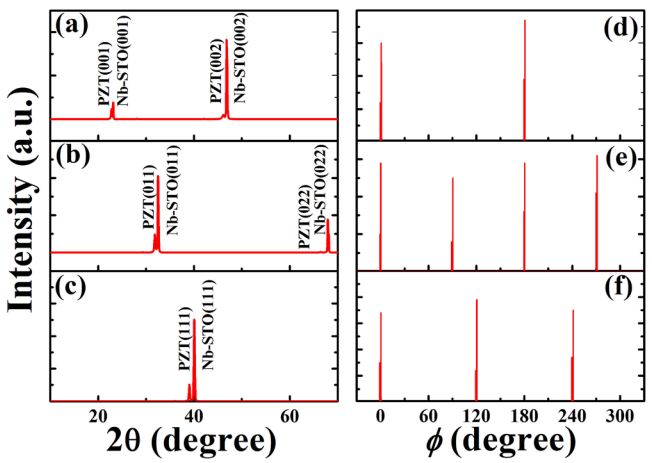

FIG. 1. XRD patterns of PZT thin films deposited on (a) (001)-, (b) (011)-, and (111)-oriented single crystal Nb-STO substrates. (d), (e), and (f) are the corresponding Φ scan, providing nonlattice-rotating epitaxial growth of PZT thin film.

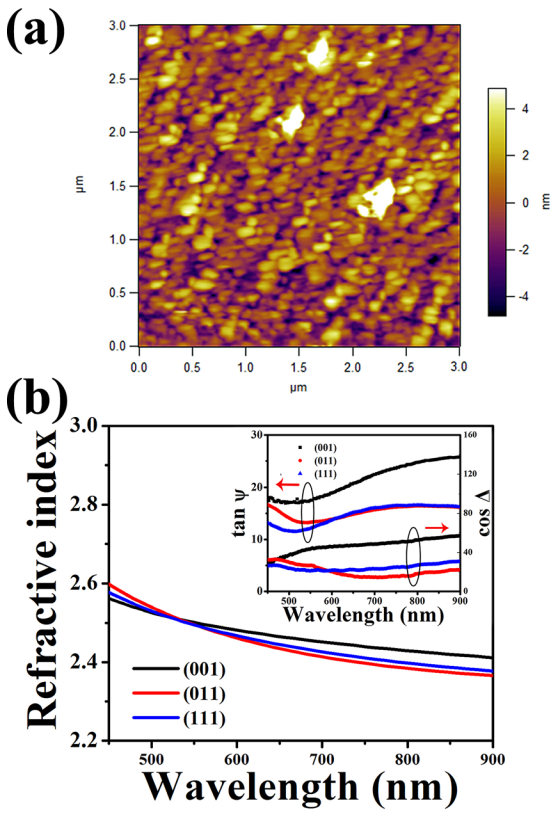

FIG. 2. (a) Surface morphology of PZT thin films from AFM. (b) Refractive index of PZT thin films with (001), (011), and (111) orientation. The inset is the original tan Ψ and cos Δ of (100)-, (011)-, and (111)-oriented PZT thin films by ellipsometry measurement.

$$n(\lambda) = A + (B/\lambda^2) + (C/\lambda^4), \tag{1}$$

where A, B, and C are the Cauchy parameters and λ is the wavelength of the incident light.[12,17] The dispersion curves rise rapidly toward shorter wavelengths, suggesting the typical shape of dispersion near an electronic inter-band transition. Conspicuous orientation dependence of refractive index is discernable, especially in near infrared region. The (001)-oriented PZT films exhibit the highest refractive indices in near IR wavelengths, while the (011)- and (111)-oriented thin films have lower refractive indices. Noted that the BO_6 octahedra in an oxygen-octahedral ABO_3 perovskite ferroelectric dominates its corresponding optical property, so the lowest energy oscillator is the largest contributor to the dispersion of the refractive index.[18] Meanwhile, voids imposed by surface roughness and porosity inside the film should also be responsible for the observed variation in refractive index of PZT thin films with different growth orientations.

The modified ellipsometric electro-optic measurement setup with a longitudinal geometry is shown in Fig. 3(a). As in the reflection geometry, an input laser beam is focused through film at an incident angle of 45° onto the top electrode. Under the applied electric field, the laser beam reflects and propagates back through the PZT thin film. Later, then an oscilloscope converts this phase shift into an intensity modulation, which is measured by a photodetector locked to the frequency of the excitation voltage. Fig. 3(b) summarizes the birefringence shift of PZT thin films with different growth orientations as a function of the applied electric field (E).

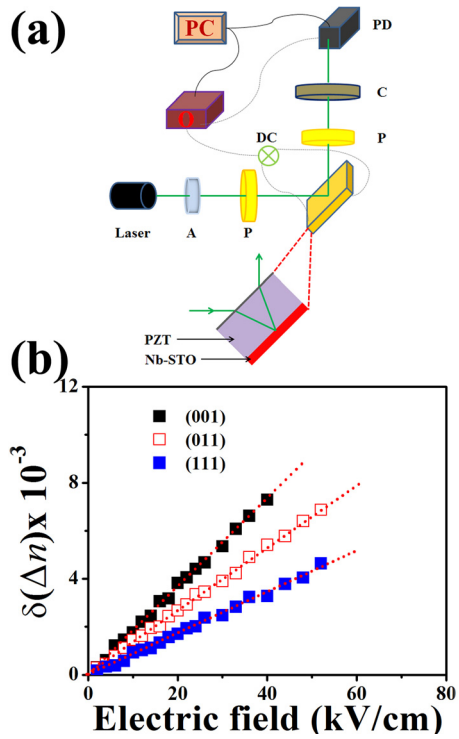

FIG. 3. Experimental setup for a reflection measurement of electro-optic coefficients: A, Attenuator; P, Polarizer; C, Compensator; PD, Photodetector; O, Oscilloscope; PC, Personal Computer; and DC, Direct Current from amplifier.(b) The birefringence $\delta(\Delta n)$ as a function of the external electrical field (E) in all three PZT thin films.

Noted that all the thin films exhibit linear EO behavior and strong orientation dependence of EO effects is clearly seen. The EO effect of (111)-oriented PZT film is relatively weak, while large birefringence changes (Δn) are observed in (001) and (011)-oriented films. The linear EO coefficient (Pockels effect) is given by[12]

$$\Delta n = -\frac{1}{2} n^3 r_c E, \tag{2}$$

where n and E are the refractive index and the applied electric field, respectively. In this case, the linear EO coefficient of the (001)-, (011)-, and (111)-oriented PZT thin films is calculated to be 270.8, 198.8, and 125.7 pm/V, respectively. The difference in EO properties in all three kinds of oriented PZT films may be attributed to the changes in distribution and magnitude of spontaneous polarization in the orientation engineered films. Further study may be needed to clarify the correction between the ferroelectric polarization, the electro-optic properties, and the crystalline orientation.

Generally, it was known that the linear electro-optic coefficient is dependent on the spontaneous polarization and dielectric constant[19,20]

$$r_{ijl} = 2P_s \varepsilon_0 (\varepsilon_{kl} - \delta_{kl}) g_{ijk} / \xi^3, \tag{3}$$

where r_{ijl}, P_s, ε_0, ε_{kl}, δ_{kl}, g_{ijk}, and ξ are the linear EO coefficient, the spontaneous polarization, the dielectric permittivity, the dielectric tensor, the Kronecker delta, the temperature independent quadratic polarization-optic coefficient of the octahedral, the packing density of the octahedral (for perovskite, $\xi = 1$), respectively. Fig. 4(a) demonstrates the dependence between the linear EO coefficient and spontaneous polarization. All PZT films, regardless of growth orientation, demonstrate symmetric, well-saturated polarization-electric field hysteresis loops (Fig. 4(a) inset). The spontaneous polarizations of all samples are 75.5, 58.0, and 40.2 μC/cm^2, respectively. It is noted that the linear EO coefficient increases as the spontaneous polarization increases, which is well agreement with the equation above. The polarization changes could originate from: (1) the magnitude variation of the relative displacement of the Ti^{4+} with respect to O^{2-}, (2) the lattice distortion by the epitaxial strain in the perovskite structure, and (3) the change of domain growth mechanism. Hence, the orientation-dependent EO behaviors of PZT thin films can be attributed to the difference of their Ti^{4+}-O^{2-} displacement when the ABO_3 structure is distorted under electrical field. Fig. 4(b) gives the schematic illustration of the nature of in-plane strain, as represented by underlying Nb-STO substrate (green) and PZT thin film (yellow). Noted that PZT film near MPB possesses a tetragonal structure with lattice parameters ($a = 4.036$ and $c = 4.146$),[16] while Nb-STO possesses a cubic phase with a = 3.905. As a result, there are two scenarios for in-plane strain, depending on the orientation of the film. For

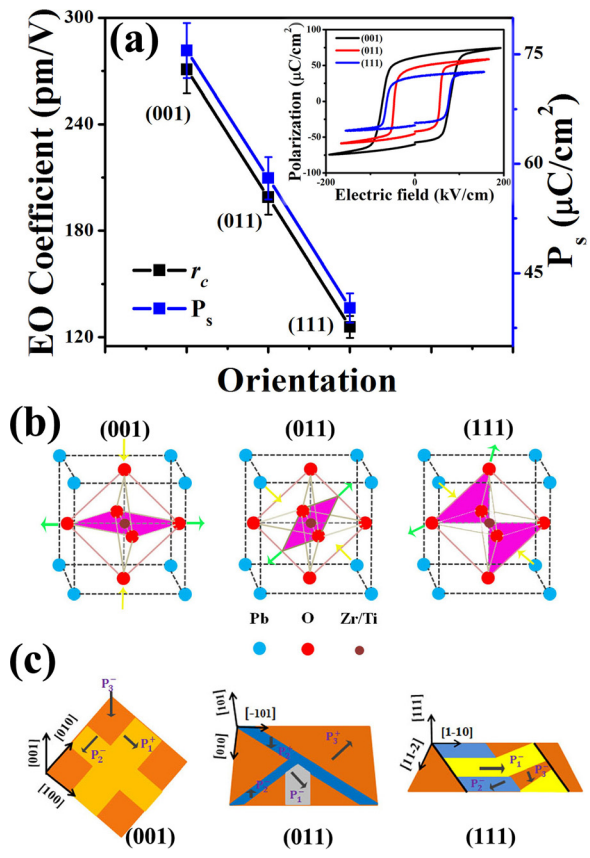

FIG. 4. (a) Relationship between the linear EO coefficient and spontaneous polarization in (001)-, (011)-, and (111)-oriented PZT thin films. The inset is polarization–electric field hysteresis loops as a function of electric field. (b) Schematic illustrations of strain application on the oxygen octahedra of the system for (001)-, (011)-, and (111)-oriented PZT thin films. (c) Schematic illustrations of the domain structures are provided for (001)-, (011)-, and (111)-oriented PZT thin films. (001)-oriented PZT films show the majority P_3^+ (orange) and minority P_1^+ and P_2^- (yellow) domains, while (011)-oriented thin films possess majority P_3^+ (orange), minority P_2^+ and P_2^- domains (blue), and small P_1^- (grey). (111)-oriented PZT films have complex nano-twinned domains with P_1^- (yellow), P_2^- (blue), and P_3^- (orange).

(001)-oriented PZT/Nb-STO heterostructures, there is a compression along the out-of-plane directions and an expansion along the in-plane direction. Similarly, (011)- and (111)-oriented samples possess both a compression and an expansion along the different octahedral faces. It can be seen that the biaxial nature of epitaxial strain could be expected to induce anisotropy in the electrical and optical properties of the PZT systems, thereby leading to anisotropic optical and EO properties. Moreover, the domain growth mechanism of PZT films maybe responsible for the obvious electro-optic anisotropy. As shown in Fig. 4(c), $P_1^{+/-}$, $P_2^{+/-}$, and $P_3^{+/-}$ represent the domains with polarization along the positive and negative [100], [010], and [001] axes, respectively. It has been found that the (001)- and (011)-oriented PZT possess a typical polydomain structure with majority $P_3^{+/-}$ domains and minority $P_1^{+/-}$ or $P_2^{+/-}$ domains, while the (111)-oriented PZT film has a complex, metastable domain pattern which consists of a high density of nanotwinned domains, thereby degenerating polarization variants.[21] Other factors such as dielectric permittivity may also be responsible for the orientation-dependent EO behaviors on our tetragonal-distorted PZT films. Nevertheless, the linear EO coefficients of (001)- and (011)-oriented PZT films are considerable higher than that of commonly used $LiNbO_3$ single crystals (~31 pm/V),[22,23] showing their potential for use in active waveguide applications.

To conclude, we have reported a strong correlation between the optical, electro-optic properties, and crystalline orientation of single crystal PZT thin films epitaxially grown on Nb-STO substrates. Through the spectroscopic ellipsometry, the refractive index of the samples exhibits a strong dependence on the growth orientation. The linear electro-optic coefficient r_c of the (001), (011), and (111)-oriented PZT thin films was found to be 270.2, 198.2, and 125.3 pm/V, respectively. Such remarkable anisotropic optical and electro-optic behaviors maybe attributed to the structure correlation between the orientation dependent distribution, spontaneous polarization, epitaxial strain, and domain pattern. Our results suggest that the (001) and (011)-oriented PZT thin films are promising for integrated optics applications.

The authors would like to acknowledge the funding support from NTU-A*STAR Silicon Technologies Centre of Excellence under the program Grant No. 1123510003 and Singapore Ministry of Education Academic Research Fund (Tier 2 Grant No. MOE2013-T2-2-050).

[1]W. W. Bruce. Annu. Rev. Mater. Res. **37**, 659 (2007).
[2]I. Vrejoiu, M. Alexe, D. Hese, and U. Gösele, Adv. Funct. Mater. **18**, 3892 (2008).
[3]D. Sando, P. Hermet, J. Allibe, J. Bourderionner, S. Fusil, C. Carrétéro, E. Jacquet, J. C. Mage, D. Dolfi, A. Barthélémy, Ph. Ghosez, and M. Bibes, Phys. Rev. B **89**, 195106 (2014).
[4]M. Veithen, X. Gonze, and P. Ghosez, Phys. Rev. Lett. **93**, 187401 (2004).
[5]S. Abel, T. Stöferle, C. Marchiori, C. Rossel, M. D. Rossell, R. Erni, D. Caimi, M. Sousa, A. Chelnokov, B. J. Offrein, and J. Formpeyrine, Nat. Commun. **4**, 1671 (2013).
[6]E. Rosenkrantz and S. Arnon, Opt. Lett. **39**, 4954 (2014).
[7]H. N. Lee, S. M. Nakhmanson, M. F. Chisholm, H. M. Christen, K. M. Rabe, and D. Vanderbilt, Phys. Rev. Lett. **98**, 217602 (2007).
[8]Y. Sakashita, H. Segawa, K. Tominaga, and M. Okada, J. Appl. Phys. **73**, 7857 (1993).
[9]G. T. Park, J. J. Choi, J. Ryu, H. Q. Fan, and H. E. Kim, Appl. Phys. Lett. **80**, 4606 (2002).
[10]K. Kurihara, M. Kondo, K. Sata, M. Ishii, N. Wakiya, and K. Shinozaki, Jpn. J. Appl. Phys., Part 1 **46**, 6929 (2007).
[11]T. D. Kang, B. Xiao, V. Avrutin, Ü. Özgür, H. Morkoç, J. W. Park, H. S. Lee, X. Y. Wang, and D. J. Smith, J. Appl. Phys. **104**, 093103 (2008).
[12]M. M. Zhu, Z. H. Du, and J. Ma, J. Appl. Phys. **108**, 113119 (2010).
[13]D. Y. Wang, S. Li, H. L. W. Chan, and C. L. Choy, Appl. Phys. Lett. **96**, 061905 (2010).
[14]Y. L. Lu, J. J. Zheng, C. G. Mark, F. L. Wang, and J. Zhao, Appl. Phys. Lett. **74**, 3764 (1999).
[15]M. Kondo, K. Sato, M. Ishii, N. Wakiya, K. Shinozaki, and K. Kurihara, Jpn. J. Appl. Phys., Part 1 **45**, 7516 (2006).
[16]N. Izyumskaya, Ya. Alivov, S.-J. Cho, H. Morkoc, H. Lee, and Y.-S. Kang, Crit. Rev. Solid State Mater. Sci. **32**, 111 (2007).
[17]M. Prabu, I. B. Shameem Banu, S. T. Sundari, R. Krishnan, K. N. Prakash, Y. C. Chen, and M. Chavali, J. Nanosci. Nanotechnol. **14**, 5335 (2014).
[18]K. Y. Chan, W. S. Tsang, C. L. Mak, and K. H. Wong, Phys. Rev. B **69**, 144111 (2004).
[19]G. H. Haertling, J. Am. Ceram. Soc. **82**(4), 797–818 (1999).
[20]C. H. Lee, V. Spirin, H. W. Song, and K. No, Thin Solid Films **340**, 242–249 (1999).
[21]R. J. Xu, S. Liu, I. Grinberg, J. Karthik, A. R. Damodaran, A. M. Rappe, and L. W. Martin, Nat. Mater. **14**, 79 (2015).
[22]Y. Takagi and K. Gesi, Jpn. J. Appl. Phys., Part 1 **5**, 1118 (1966).
[23]M. Roussey, M.-P. Bernal, N. Courjal, D. Van Labeke, F. I. Baida, and R. Salut, Appl. Phys. Lett. **89**, 241110 (2006).